Reaction of Bisphenol A with Synthetic and Commercial $MnO_{x(s)}$: Spectroscopic and Kinetic Study

Journal:	*Environmental Science: Processes & Impacts*
Manuscript ID	EM-ART-03-2018-000121.R2
Article Type:	Paper
Date Submitted by the Author:	18-May-2018
Complete List of Authors:	Shaikh, Nabil; University of New Mexico, Civil Engineering Zhang, Huichun; Case Western Reserve University Case School of Engineering, Department of Civil Engineering Rasamani, Kowsalya Devi; Temple University, Department of Chemistry Artyushkova, Kateryna; University of New Mexico, Chemical and Nuclear Engineering Ali, Abdul-Mehdi; University of New Mexico, Earth and Planetary Sciences Cerrato, Jose; University of New Mexico, Civil Engineering

Environmental Science: Processes & Impacts

PAPER

Reaction of Bisphenol A with Synthetic and Commercial $MnO_{x(s)}$: Spectroscopic and Kinetic Study

Received 16th March 2018,
Accepted 00th January 20xx

DOI: 10.1039/x0xx00000x

www.rsc.org/

Nabil Shaikh[a*], Huichun Zhang[b,c], Kowsalya Rasamani[c], Kateryna Artyushkova[d], Abdul-Mehdi S. Ali[e], and José M. Cerrato[a]

The reaction of bisphenol A (BPA) using laboratory synthesized (Syn-MnO_x) and commercially available (Com-MnO_x) $MnO_{x(s)}$ media was investigated using spectroscopic and aqueous chemistry methods. The surface area of Syn-MnO_x (128 m^2/g) and Com-MnO_x (13.6 m^2/g) differed by an order of magnitude. The impurities were less than 1% by weight for Syn-MnO_x while Com-MnO_x contained 29% impurity by weight, mainly Al, Si and Fe. The removal of 99.7% BPA was observed applying Syn-MnO_x, while 71.2% BPA removal was observed applying Com-MnO_x after 44 hours of reaction of 10 mM $MnO_{x(s)}$ media with 1mM BPA at pH 5.5. The reduction of Mn was detected in the surface of both BPA reacted media, but a higher content of reduced Mn was observed in Syn-MnO_x (52% in Syn-MnO_x compared to 29% in Com-MnO_x). The release of soluble Mn was an order of magnitude higher in batch experiments reacting BPA with Syn-MnO_x compared with Com-MnO_x. The C 1s and O 1s XPS high resolution spectral analyses identified the presence of functional groups that likely correspond to BPA oxidation products, such as dimers and quinones associated with $MnO_{x(s)}$ surfaces on both reacted media. The reaction of BPA with Syn-MnO_x fit the electron transfer-limited model (R^2=0.96), while the reaction of BPA with Com-MnO_x had a better fit for surface complex formation-limited model (R^2=0.95). These results suggest that BPA removal and the reactivity of $MnO_{x(s)}$ are affected by the differences in surface area and impurities present in these media. Thus, this study has relevant implications for the reaction of $MnO_{x(s)}$ with emerging organic contaminants in natural biogeochemical processes and water treatment applications.

Environmental Significance:
The reactivity of manganese oxides [$MnO_{x(s)}$] is relevant to the fate and transport of emerging micropollutants in natural and engineered systems. The limited current knowledge on the reaction of bisphenol-A (BPA) with synthetic-MnO_x and commercial-MnO_x motivates this study. The results from this research suggest that the reaction of BPA with synthetic-MnO_x fit the electron transfer limited model, while the reaction of BPA with commercial-MnO_x had a better fit with the surface complex formation limited model. The physicochemical differences between synthetic-MnO_x and commercial-MnO_x affect the observed variations in the interfacial interaction of these solids with BPA. The findings from this study are relevant to better understand biogeochemical processes affecting the reaction of emerging organic micropollutants with $MnO_{x(s)}$ in natural systems, and potential applications for water treatment.

Introduction

Compounds classified as endocrine disruptors such as organic micropollutants are a major concern in natural and engineered water systems. These contaminants, even in trace levels, have been shown to have adverse effects on aquatic communities.[1,2] Bisphenol A (BPA) is an example of a micropollutant that was widely used as a plasticizer in the polymer production industries and has been found to be estrogenically active.[3] The incomplete removal of BPA at existing wastewater and drinking water treatment plants is a concerning issue due to its estrogenic activity.[4,5] Thus, the identification of geochemical processes affecting the reaction of these micropollutants is necessary to understand the fate of these chemicals and develop economically efficient treatment technologies.

Previous studies [6–8] have shown that organic micropollutants react with $MnO_{x(s)}$ resulting in reductive dissolution of Mn and oxidation of organic groups. Recent studies [9–12] have shown that the oxidation rate of organic micropollutants reacted with $MnO_{x(s)}$ decreases in the presence of secondary metal oxides, metal cations and natural organic matter. The use of

[a] Department of Civil Engineering, MSC01 1070, University of New Mexico, Albuquerque, New Mexico 87131, USA.
[b] Department of Civil Engineering, Case Western Reserve University, 10900 Euclid Avenue, Cleveland, OH 44106, USA.
[c] Department of Civil and Environmental Engineering, Temple University, 1947 N. 12th Street, Philadelphia, PA 19122, USA.
[d] Department of Chemical & Biological Engineering, MSC01 1120, 1 University of New Mexico Albuquerque, NM 87131, USA.
[e] Department of Earth and Planetary Sciences, MSC03 2040, University of New Mexico, Albuquerque, New Mexico 87131, USA.
* E-mail: mnabilshaikh@unm.edu
Electronic Supplementary Information (ESI) available: additional description of experimental setup, XPS, SEM/EDS, and XRF data. See DOI: 10.1039/x0xx00000x

commercially available $MnO_{x(s)}$ derived from natural $MnO_{x(s)}$ minerals is well documented in water treatment for inorganic contaminant removal.[13–16] However, only a few studies have been done to evaluate the feasibility of using these commercial $MnO_{x(s)}$ for the removal of organic compounds.[17,18] Recent studies have shown promising results in the application of $MnO_{x(s)}$ in columns and bed filters for removal of pharmaceuticals such as diclofenac and estradiols via biotic and abiotic mechanisms.[19–22] Additionally, the effect of surface area and surface impurities on reactivity of $MnO_{x(s)}$ with organic micropollutants is not well understood as most studies utilize pure synthesized media that are not completely representative of naturally occurring manganese oxides.[11,23,24] The effect of $MnO_{x(s)}$ surface physicochemical properties on the media performance and contaminant removal kinetics is of utmost importance to determine the fate and transport of these contaminants in natural and engineered systems.[20] However, limited investigations have compared the differences in reaction of organic micropollutants with commercial versus synthetic $MnO_{x(s)}$.

The objective of this study was to evaluate the reaction of BPA by laboratory synthesized (Syn-MnO_x) and commercially available (Com-MnO_x) $MnO_{x(s)}$ media using spectroscopic and aqueous chemistry techniques. We monitored solid phase changes based on the Mn oxidation state of $MnO_{x(s)}$, C1s and O1s bonding using X-ray photoelectron spectroscopy (XPS), while residual BPA and soluble Mn were evaluated to obtain the kinetics of BPA removal. The physicochemical difference in Syn-MnO_x and Com-MnO_x media employed in this study provided an interesting basis for comparison of the reactivity of each media with BPA. Given that commercially available media are economically affordable, the results from this study provide insights into the practical application of $MnO_{x(s)}$ for treatment of organic micropollutants in engineered systems.

Materials and methods

Materials

Bisphenol A (>99% purity) was purchased from Sigma Aldrich (St. Louis, MO). Commercial MnO_x (Com-MnO_x, LayneOx® media purchased from Layne Co., TX) is a $MnO_{x(s)}$ filter media, which is used to remove inorganics from drinking water such as Mn and Fe.[13,25,26] Pure (>99%) manganese oxides (MnO, Mn_2O_3, MnO_2 and Mn(III,IV) oxide) were purchased from Strem Chemicals (Newburyport, MA) and Sigma Aldrich (St. Louis, MO) to be used as XPS references. All other chemicals where bought from VWR or Thermo Fisher with >90% purity and used without further purification. The Syn-MnO_x was synthesized as described by Taujale and Zhang [11,12] reacting $KMnO_4$ and $MnCl_2$ in basic conditions to precipitate as Mn(III)-rich δ-$MnO_{x(s)}$.

Batch experiments

The reaction of BPA with $MnO_{x(s)}$ was studied to examine the impacts of solutes and impurities on the removal of BPA and net release of manganese into solution. First, batch experiments were conducted with 1 mM BPA reacting with 10 mM Syn-MnO_x or 10 mM Com-MnO_x (in separate reactors) in ultrapure water at pH 5.5 (buffered using 50 mM phosphate buffer). A concentration of 0.01 M NaCl was added to the reactors to maintain ionic strength. The pH 5.5 was chosen to keep the study at conditions relevant for engineered systems while remaining low enough for the reaction to be appreciably completed within the experimental time-frame. Elevated concentrations of BPA and $MnO_{x(s)}$ were used to have appreciable amounts of BPA reacted solids collected for analyses during the experimental time-frame. The reactor setup is shown in supporting information (Figure S1). A volume of 10 ml of liquid samples were filtered through 0.45 µm and taken at timed intervals (5, 15, 30, 45, 90, 180 minutes and 44 hours) to evaluate the dissolved Mn and residual BPA. The $MnO_{x(s)}$ media in the reactors were used for solid phase analysis.

Adsorption/oxidation experiments

The reactors for kinetic experiments were set up in 60 ml screw-cap amber bottles with Teflon caps. The reaction was carried out under similar reactor conditions to the batch experiment described above. Reactors with 100 µM of Syn-MnO_x or Com-MnO_x were setup and 10 µM of BPA was added to the reactors to initiate the reaction at pH 5.0 using 25mM acetate buffer. Samples were taken at predetermined time intervals with two different approaches to quench the reaction. The first approach was to centrifuge and filter through a 0.22 µm filter and the second approach was using NaOH in order to increase pH to above 10.0 followed by centrifuging and filtering the sample. Although we did not show the results in this work, in our separate research on BPA oxidation by $MnO_{x(s)}$, ascorbic acid was used to quench the reaction and comparable kinetics were observed using both quenching methods. Previous work has shown that phenolic compounds stop oxidizing and completely desorb from $MnO_{x(s)}$ surface at high pH values.[11,12,27] The aliquots were analyzed for residual BPA using high performance liquid chromatography (HPLC).

Solid phase analysis

The surface area was calculated using N_2 adsorption (Brunauer–Emmett–Teller) on a Micrometrics 2360 Gemini Analyzer. The bulk elemental composition of the $MnO_{x(s)}$ media were analyzed using Energy-dispersive X-ray spectroscopy (EDS) and X-ray Florescence (XRF). A Kratos Axis DLD Ultra X-ray photoelectron spectrometer with a monochromatic Al Kα source was used to acquire the XPS spectra at 225W with no charge compensation from three different areas on each sample. Elemental survey spectra were acquired at 80 eV and high resolution at 20 eV pass energy. The software CasaXPS was used to perform curve fitting and quantification. XPS spectra were processed using Shirley background subtraction and a Gaussian-Lorentzian line shape for the curve fitting.[25] Oxidation states of Mn were determined using the Mn 3s multiplet splitting method and by examination of the shape and position of the Mn 3p region as described by Cerrato et

al.[25,28] Analyses of O 1s and C 1s spectra were done based on results obtained from other studies.[6,24]

Liquid phase analysis

A reverse phase HPLC with an electro-chemical detector was used to analyze BPA in liquid samples of batch experiments. A TSKgel ODS-80Tm C-18 column (4.6×250 mm, 5 µm) was used with a mobile phase of 50% methanol, 50% phosphate buffer at pH 6 and a flowrate of 0.8 ml/min. The peak for BPA was obtained at around 10 min retention time. A Perkin-Elmer Nexion 300D inductively coupled plasma-mass spectrometer (ICP-MS) system was used to analyze the metal concentration in liquid samples from the reactor.

Kinetic analysis

The reaction between $MnO_{x(s)}$ and BPA is assumed to follow the kinetic models developed in a previous study:[29]

$$MnO_x(s) + \text{BPA} \underset{k_{-1}}{\overset{k_1}{\rightleftharpoons}} (MnO_x - \text{BPA}) \underset{k_{-2}}{\overset{k_2}{\rightleftharpoons}} (> Mn^{III}, \text{BPA}^{\bullet}) \xrightarrow{fast} Mn^{2+} + \text{BPAO}^{*}$$

Briefly, the reaction initiates with formation of an organic reactant - oxide surface precursor complex (MnO_x–BPA), followed by electron transfer in the complex resulting in organic radical formation and surficial Mn reduction (>Mn^{III}, BPA•). The reaction proceeds with rapid transformation of the unstable organic radical resulting in formation of BPA oxidation products (BPAO*) and further reduction of surficial Mn to soluble Mn^{2+}. The kinetic model equation varies based on the rate limiting step: (i) limited by electron transfer, and (ii) limited by precursor surface complex formation. The analytical solution for each scenario is as follows:

(i) Electron transfer limited:

$$C = C_e + S_{rxn} \cdot e^{-k' \cdot t} \; ; \; k' = k_2$$

(ii) Surface complex formation limited:

$$1 - \frac{C_e}{C} = \frac{S_{rxn}}{C_o} \cdot e^{-k'' \cdot C_e \cdot t} \; ; \; k'' = \frac{k_1 \cdot k_2}{k_{-1} + k_2}$$

Where, *C* is the molar concentration of the BPA in the reactor with subscripts '*0*' and '*e*' representing initial and equilibrium concentration respectively, *t* is time in hours, *k' (h^{-1}) and k" (h^{-1} M^{-1})* are the rate constants, and S_{rxn} is the total reactive surface sites that can be oxidized by BPA, calculated as $S_{rxn} = C_o - C_e$.

Results and discussion

Physical and chemical characterization of $MnO_{x(s)}$

The surface area measured by BET was one order of magnitude higher for Syn-MnO_x (128.3 m^2/g) compared to Com-MnO_x (13.6 m^2/g). Bulk elemental analyses conducted on the unreacted Com-MnO_x media using XRF show that Al (10%), Fe (9 %) and Si (7%) are the most abundant impurities in the which had an Mn content of 71% (Table S1). A content of 99.9% Mn and no detectable metal impurities were observed for Syn-MnO_x based on the XRF and EDS analyses.

Near surface elemental composition. The presence of impurities was observed in the top 5-10 nm (near surface) by XPS survey scans for unreacted (control) and BPA-reacted media (Com-MnO_x and Syn-MnO_x) (Table 1). The carbon content (C 1s) for control Com-MnO_x was 50.8% and for control Syn-MnO_x was 39.1%, likely due to the contribution of adventitious carbon. In contrast, there was an increase in C 1s for both reacted Com-MnO_x (60.9%) and reacted Syn-MnO_x (60.4%), suggesting the possible association of organic compounds to the $MnO_{x(s)}$ surface. The presence of Al and Si was detected in the surface of control and reacted Com-MnO_x samples, confirming the presence of impurities in these media as indicated by the XRF and EDS analyses. A decrease in Al 2p in the surface of reacted Com-MnO_x samples (2.8%) compared to 4.2% in control Com-MnO_x samples was observed, which also suggests a decrease on the Al signal due to the presence of organic compounds in the surface of $MnO_{x(s)}$. A decrease in Mn 2p signal is observed in Syn-MnO_x, from 11.7% in control Syn-MnO_x to 6.2% for reacted Syn-MnO_x. The Mn 2p content in the control Com-MnO_x sample (1.9%) showed a minor decrease when reacted with BPA, 1.4% for the reacted Com-MnO_x samples. Additional aqueous samples from the batch experiments of BPA reaction with $MnO_{x(s)}$ media were analyzed to obtain information on BPA removal and Mn dissolution.

Table 1. Near surface elemental composition of synthetic (Syn-MnOx) and commercial (Com-MnOx) manganese oxide media after reaction with BPA. Uncertainty shown is standard deviation for triplicate data.

	C 1s %	O 1s %	Mn 2p%	Si 2p %	Al 2p %
Syn-MnO_x Control	39.1 ± 4.3	49.2 ± 3.1	11.7 ± 1.2	-	-
Syn-MnO_x Reacted	60.4 ± 0.3	33.4 ± 0.2	6.2 ± 0.1	-	-
Com-MnO_x Control	50.8 ± 3.0	40.0 ± 1.5	1.9 ± 0.2	3.1 ± 0.7	4.2 ± 0.6
Com-MnO_x Reacted	60.9 ± 5.2	31.7 ± 3.9	1.4 ± 0.4	3.2 ± 0.3	2.8 ± 1.0

Residual BPA

Higher amount of residual BPA was observed when reacted with Com-MnO_x (0.228 mM BPA) compared to Syn-MnO_x (0.002 mM BPA) in the batch experiments (Figure 1). No BPA

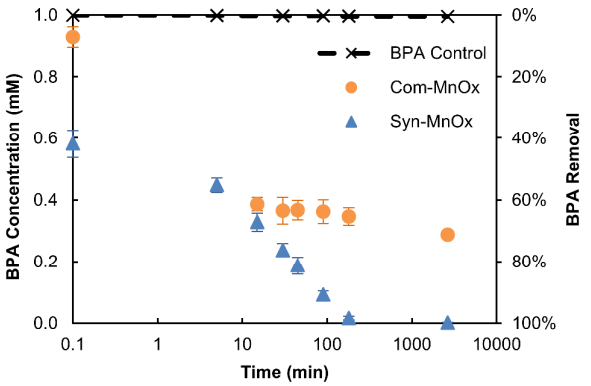

Fig. 1. Residual BPA concentrations in aliquots from batch experiments of solutions reacted with Commercial MnO_x (circle) and Synthesized MnO_x (triangle) taken at times 0.1, 5, 15, 30, 45, 90, 180 and 2640 mins. Reaction conditions were 10 mM MnO_x, 1 mM BPA, 10 mM NaCl and pH 5.5, vertical error bars represent standard deviation for triplicate reactors.

removal was observed for control experiments conducted in the presence of BPA and absence of $MnO_{x(s)}$. Rapid initial BPA removal was observed for Syn-MnO_x (67% removal) and Com-MnO_x (61% removal) during the first 15 mins. As the reaction proceeded from 15 mins onwards, BPA removal followed first order kinetics with rates of 0.096 hr^{-1} for Syn-MnO_x and 0.0054 hr^{-1} for Com-MnO_x. Faster removal of BPA was observed for Syn-MnO_x while slower for Com-MnO_x. The residual BPA data was used in the kinetic analyses presented later.

Our data from adsorption/oxidation experiments suggest that removal of BPA was mainly due to oxidation in the case of Com-MnO_x, while Syn-MnO_x had retained un-oxidized BPA on its surface, which was released by addition of excess NaOH (Figure 2). Thus, removal of BPA was likely due to adsorption followed by rapid oxidation on the $MnO_{x(s)}$ media. The maximum amount of BPA removed solely by adsorption on $MnO_{x(s)}$ was calculated to be 32 µM BPA per mM MnO_x for Syn-MnO_x and 3.3 µM BPA per mM MnO_x for Com-MnO_x. This maximum amount was calculated by extrapolating the data of total BPA removed subtracted from BPA removed solely by oxidation (Figure S2). As the reaction proceeded, the amount of BPA removed by adsorption onto the media decreased linearly with respect to time and residual BPA concentration, most likely due to the continuous oxidation of the adsorbed BPA. The concentration of adsorbed BPA at the end of 4 hours was 0.44 µM for Syn-MnO_x and 0.08 µM for Com-MnO_x.

Differences in the BPA removal and BPA adsorption kinetics can be attributed to the differences in surficial properties, as the presence of impurities results in fewer reactive sites available for BPA oxidation. For instance, the Syn-MnO_x has 99.9% purity. However, Com-MnO_x has 29.1% impurities which likely occupy surface sites with elements such as Al and Si as indicated by XPS survey scans (Table 1). The release of soluble Mn during the reaction was studied to further understand the influence of surface chemistry and differences in the reactivity between the $MnO_{x(s)}$ media.

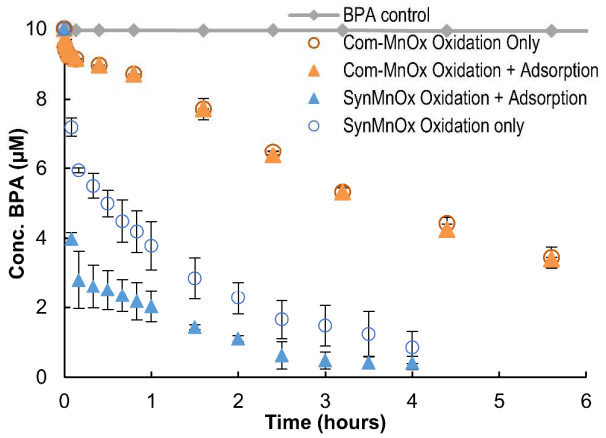

Fig. 2. Residual BPA in the reactors after reaction with MnOx(s) media; Syn-MnOx (blue) and Com-MnOx (orange). The samples were treated in two ways, by only filtering to get removal by oxidation and adsorption (solid triangle), or by adding NaOH to get BPA removed by oxidation alone (hollow circle). Reaction conditions: 100 µM MnOx, 10 µM BPA, 10 mM NaCl, pH 5.0, vertical error bars represent standard deviation for duplicate reactors.

Soluble Mn release to solution

The soluble Mn released to solution due to Mn dissolution after 44 hours of reaction of $MnO_{x(s)}$ with BPA in the batch experiments was one order of magnitude higher for Syn-MnO_x (14.2 mg/l) than Com-MnO_x (1.7 mg/l). Both Syn-MnO_x and Com-MnO_x media that reacted with BPA showed a similar initial soluble Mn concentration of 0.25 mg/l at 5 mins. After 44 hours of reaction, the final Mn release value of 14.2 mg/l was obtained for Syn-MnO_x, compared to 1.1 mg/l for Com-MnO_x (Figure 3). It is likely that the differences in surficial properties, such as lower surface area influenced the limited Mn dissolution observed in Com-MnO_x when compared to Syn-MnO_x. As the reaction proceeds, the $MnO_{x(s)}$ surface sites are occupied by oxidation products and consumed due to Mn reduction. Thus, we observed two distinct and opposite trends in the BPA removal and soluble Mn release: a) an initial rapid BPA removal corresponding with low soluble Mn release; and b) later, a slower BPA removal and high Mn release.

The order of magnitude difference in Mn release for the two media is comparable to the order of magnitude difference in the surface area of the two media. On normalizing the Mn release to respective surface area, the amount of Mn released was within 2% for both media (0.11 mg/l Mn per unit surface area for Syn-MnO_x and 0.13 mg/l Mn per unit surface area for Com-MnO_x). Thus, these data suggest that the availability of surface binding sites is essential for the oxidation of BPA and subsequently, for re-adsorption/re-oxidation of aqueous Mn onto $MnO_{x(s)}$, as suggested in other studies.[7,11,24] Additional analyses were carried out to understand the influence of interfacial processes at the $MnO_{x(s)}$ surface on the reaction with BPA, such as change in Mn oxidation state and carbon/oxygen bonding in the near surface of $MnO_{x(s)}$.

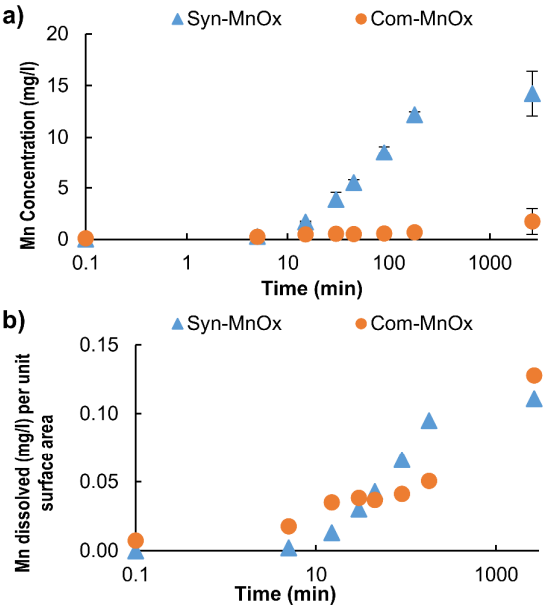

Fig. 3. (a) Concentration of Mn released into solution from batch experiments (n=3) and (b) Mn release normalized to surface area of respective media for Syn-MnO_x (triangle) and Com-MnO_x (circle). Reaction conditions were 10 mM MnO_x, 1 mM BPA, 10 mM NaCl and pH 5.5, vertical error bars represent standard deviation for triplicate reactors.

Oxidation state of Mn

The presence of more than 75% Mn(IV) and less than 25% Mn(III) was observed in the near surface region of unreacted $MnO_{x(s)}$, and the reduction of Mn after reaction with BPA was determined by XPS analyses of Mn 3s multiplet splitting and Mn 3p spectra. The data shows an increase in Mn 3s multiplet splitting values for reacted Syn-MnO_x (4.82) compared to 4.63 for control Syn-MnO_x, and a similar increase for reacted Com-MnO_x (4.68) compared to 4.47 for control Com-MnO_x (Table S2). The value of 4.82 for reacted Syn-MnO_x is within 0.08 eV of the Mn(III, IV) reference and the value of 4.47 for control Com-MnO_x is within 0.09 eV of the Mn(IV) reference. The increase in multiplet splitting for the reacted samples suggests reduction in the Mn oxidation state of $MnO_{x(s)}$ occurred after reaction with BPA. On comparison with the Mn reference data, the average surface Mn oxidation state for control Syn-MnO_x was 3.7 and for control Com-MnO_x was 3.9, consistent with data from other studies of 3.6 to 3.9 for unreacted birnessite.[7,24,30] The average Mn oxidation state for reacted Syn-MnO_x was 3.5 (compared to 3.7 for unreacted Syn-MnO_x) and for reacted Com-MnO_x was 3.7 (compared to 3.9 for unreacted Com-MnO_x), which indicated reduction of Mn on the surface.

The presence of reduced Mn is confirmed by the change of the shape of the Mn 3p spectra, which show more pronounced shoulders that correspond with the reduced Mn references (Figure 4). The contribution of Mn(IV) to Mn 3p spectra decreased in reacted samples, while the shoulder features that correspond to reduced Mn increased. For example, the control Syn-MnO_x (73%) had more Mn(IV) than the reacted Syn-MnO_x (48%); a similar trend was observed for the control Com-MnO_x (88%) compared to the reacted Com-MnO_x reacted (71%). An increase in reduced Mn features was observed in the Mn 3p spectra of reacted $MnO_{x(s)}$ samples, with 22% increase in Mn(III) characteristics for reacted Syn-MnO_x compared to control Syn-MnO_x and 14% increase in Mn(III) characteristics for reacted Com-MnO_x compared to control Com-MnO_x. Negligible Mn(II) was observed in the control samples; but a minor presence of Mn(II) in the reacted $MnO_{x(s)}$ samples was identified in both media [reacted Syn-MnO_x had 4% Mn(II) and reacted Com-MnO_x had 3% Mn(II)]. The average oxidation states calculated from Mn 3p were similar to the oxidation state calculated from Mn 3s multiplet splitting values. Thus, the presence of reduced Mn in $MnO_{x(s)}$ from XPS analyses and the increasing presence of soluble Mn in solution confirm that the reductive dissolution of $MnO_{x(s)}$ occurred in these experiments. Additional XPS analyses were conducted to assess changes in the C 1s and O 1s high resolution spectra after reaction with BPA.

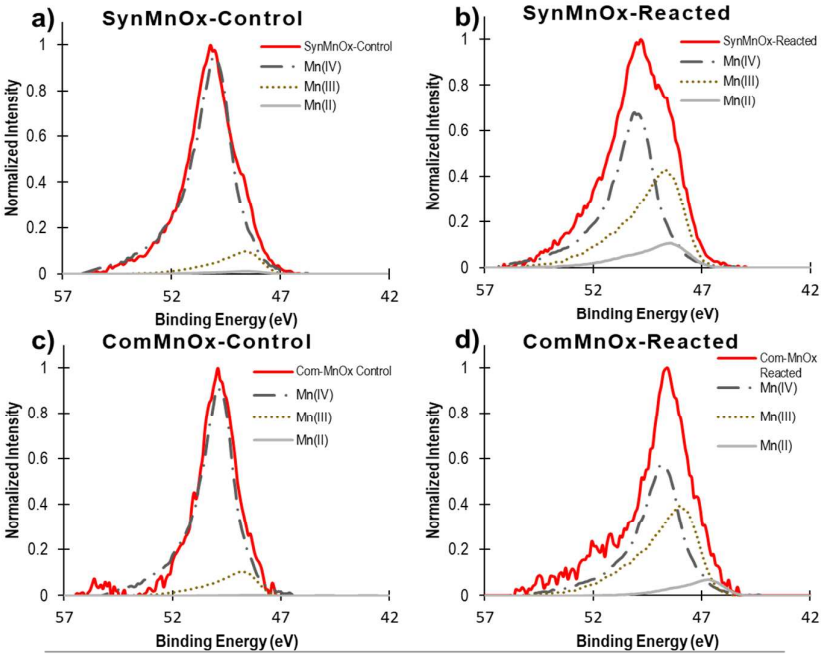

e)

Sample	% Mn IV	% Mn III	% Mn II	Oxidation state
Syn-MnO_x Control	73 ± 3	26 ± 3	1 ± 0.5	3.7
Syn-MnO_x Reacted	48 ± 5	48 ± 4	4 ± 0.7	3.4
Com-MnO_x Control	88 ± 2	12 ± 2.4	0 ± 0.2	3.9
Com-MnO_x Reacted	71 ± 6	26 ± 7	3 ± 0.6	3.7

Fig. 4. High resolution Mn 3p fitted spectra for $MnO_{x(s)}$ media (a) unreacted Syn-MnO_x (b) Syn-MnO_x reacted with BPA (c) unreacted Com-MnO_x (d) Com-MnO_x reacted with BPA; (e) Percent composition of Mn 3p spectra by fitting Mn(II), Mn(III) and Mn(IV) reference spectra, uncertainty shown is standard deviation for triplicate data. Note that the spectra for unknown samples are shown in red, and for the Mn(II), Mn(III), and Mn(IV) references are shown in grayscale.

Oxygen and carbon surface bonding

The changes in the shapes of the O 1s and C 1s high resolution XPS scans for both Syn-MnO_x and Com-MnO_x suggest that the binding environments of oxygen and carbon changed after the reaction with BPA. The analysis and fitting of O 1s spectra for unreacted and reacted $MnO_{x(s)}$ media are illustrated in Figure 5 and the relative percentage composition of corresponding oxygen bonds are summarized in Table S3. The presence of peaks associated with organic oxygen bonds on the surface of control samples can be attributed to adventitious contamination. There is a decrease in the peak at 529.6 eV which corresponds to oxygen species attached to metal, from 59.4% in the Syn-MnO_x control to 33.0% in reacted Syn-MnO_x. A decrease in the same peak (529.6 eV) is observed from 17.2% in control Com-MnO_x to 13.7% in reacted Com-MnO_x. An approximate 10% increase in O 1s component at 533.7 eV, associated with oxygen from esters/carboxylates (C-O-C/COOH), was observed in the reacted MnO_x samples for both media, with reacted Syn-MnO_x 17.7% compared to control Syn-MnO_x 7.9% and reacted Com-MnO_x 30.0% compared to control Com-MnO_x 22.1%. Additionally, presence of a noticeable peak at 535 eV was observed on reacted MnO_x media, which is attributed to the presence of C-O-O-C bonds.

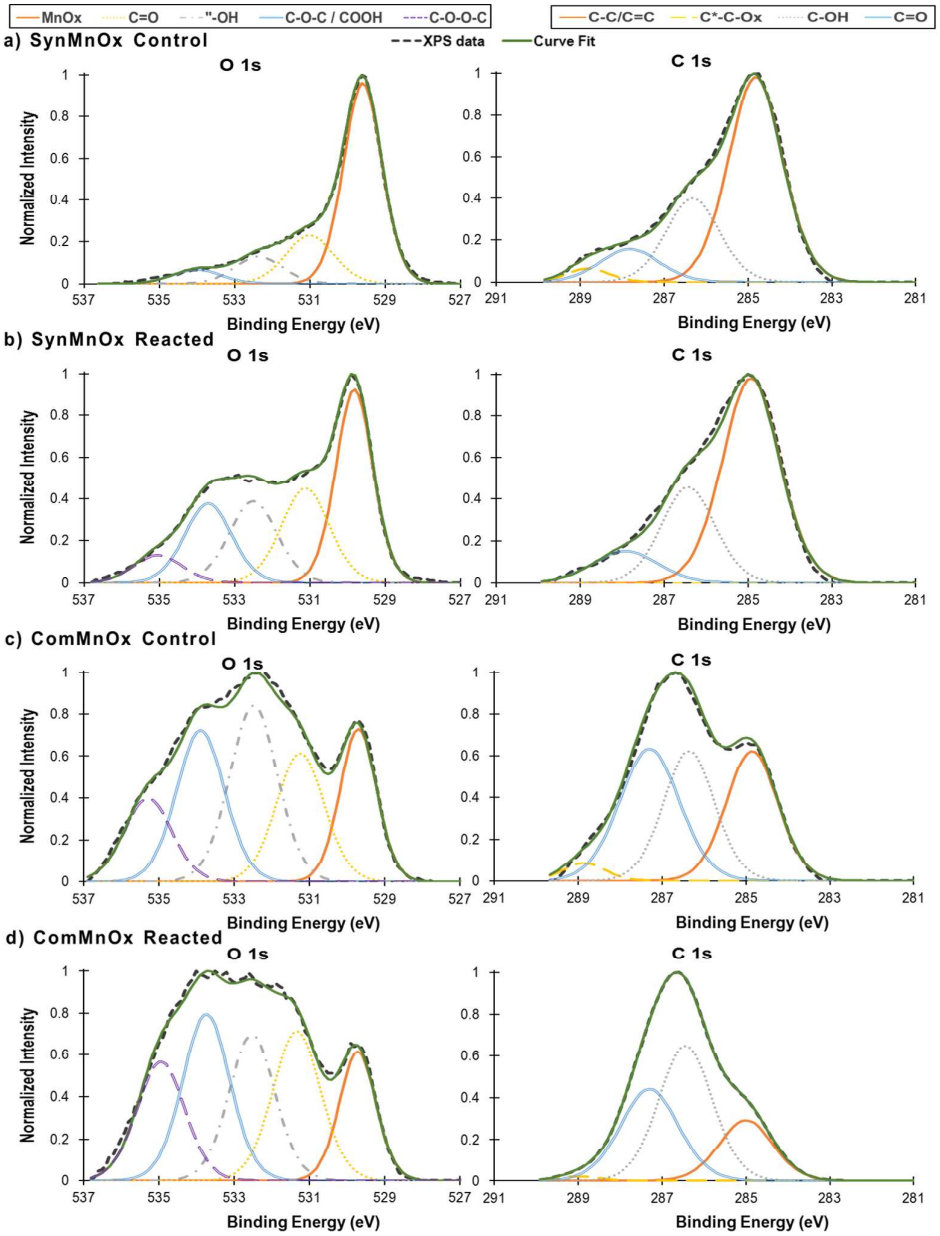

Fig. 5. High resolution XPS O 1s (left) and C 1s (right) fitted spectra with corresponding types of oxygen and carbon bonds based on their binding energy for (a) Syn-MnO_x-control, (b) Syn-MnO_x-reacted, (c) Com-MnO_x-control, and (d) Com-MnO_x-reacted. The XPS data are shown as black dotted lines, solid green lines represent the composite curves of these bonds, and the different component oxygen or carbon bonds are shown as inset lines.

Fits to the O 1s spectra for reacted Syn-MnO_x suggest the presence of 5.3% C-O-O-C bonds; the reacted Com-MnO_x contained 21.6% C-O-O-C bonds compared to 12.5% in the control Com-MnO_x. No features characteristic to C-O-O-C bonds were observed in the control Syn-MnO_x. The increase in peaks associated with other oxygen bonds, such as C–O–O–C, and C–O–C, indicates association of organic groups with the $MnO_{x(s)}$ surface such as dimers and quinones, which are formed due to radical coupling during the oxidation of phenolic compounds by $MnO_{x(s)}$.[10,23] The increased contribution of peaks associated with these organic groups suggests that adsorbed BPA oxidation products are present in the $MnO_{x(s)}$ surface even after completion of the reaction.

The changes in C1s spectra after the reaction of $MnO_{x(s)}$ with BPA suggest that aromatic organic reaction products are associated with the solid surface. The C1s spectral analyses are illustrated in Figure 5 and the fitting of these spectra to identify features that correspond to different carbon bonds is shown in Table S4. The C-C/C=C bonds (characteristic binding energy 284.8 eV) are associated with adventitious carbon [6,24] and were present in similar amounts at 63.4% for reacted Syn-MnO_x vs. 65.2% for control Syn-MnO_x, and 26.4% for reacted Com-MnO_x vs. 34.7% for control Com-MnO_x. Similarly, the peaks at the binding energy 288.5 eV, associated with C=O bonds, were within 2% of each other for reacted and control samples (reacted Syn-MnO_x has 9.7% C=O bonds compared to 9.2% control Syn-MnO_x, and reacted Com-MnO_x has 31.5% C=O bonds compared to 29.1% control Com-MnO_x). An increase was observed in the peak at 287.2 eV associated with C-OH bonds, (reacted Syn-MnO_x has 26.6% compared to 21.2% control Syn-MnO_x; and reacted Com-MnO_x has 40.9% compared to 33.0% control Com-MnO_x). Both reacted Syn-MnO_x and reacted Com-MnO_x show a decrease (4%) in C 1s component at binding energy 285.6 eV which are associated with secondary carbon carboxylates when compared to the control. This decrease in -COOH and increase in -COH indicates decarboxylation of BPA and retention of aromatic compounds on the surface of $MnO_{x(s)}$, as observed in other studies.[21,31] The formation of dimers and decarboxylation can explain sorption onto the media due to reduced electrostatic repulsion with the $MnO_{x(s)}$ surface.[21] Additional kinetic analyses were conducted to evaluate possible pathways that affect BPA removal by Syn-MnO_x and Com-MnO_x.

Kinetic analyses

The results of fitting the kinetic data (illustrated in Figure 6) for (i) electron transfer limited model (k') and (ii) surface complex formation limited model (k"), show that the rate limiting step in the reaction of BPA with Syn-MnO_x is most likely electron transfer. This finding is similar to previous studies between pure $MnO_{x(s)}$ and phenolic compounds.[7,23,29] The data for BPA reaction with Syn-MnO_x adequately fit to the electron transfer-limited model (R^2=0.96), with the calculated rate constant of k' = 1.25 h^{-1} for the electron transfer limited transformation of BPA by $MnO_{x(s)}$.

The prescribed model for surface complex formation limited reaction yielded a better fit for Com-MnO_x (k" = 0.45 mM^{-1} h^{-1}, R^2 = 0.95) compared to the electron transfer limited model (R^2=0.86). The poor fit for Com-MnO_x electron transfer limited model could be due to the presence of impurities (e.g., Al, Si, Fe) on the solid surface which may influence the kinetics of the reaction. For instance, oxides of Al and Fe have a strong

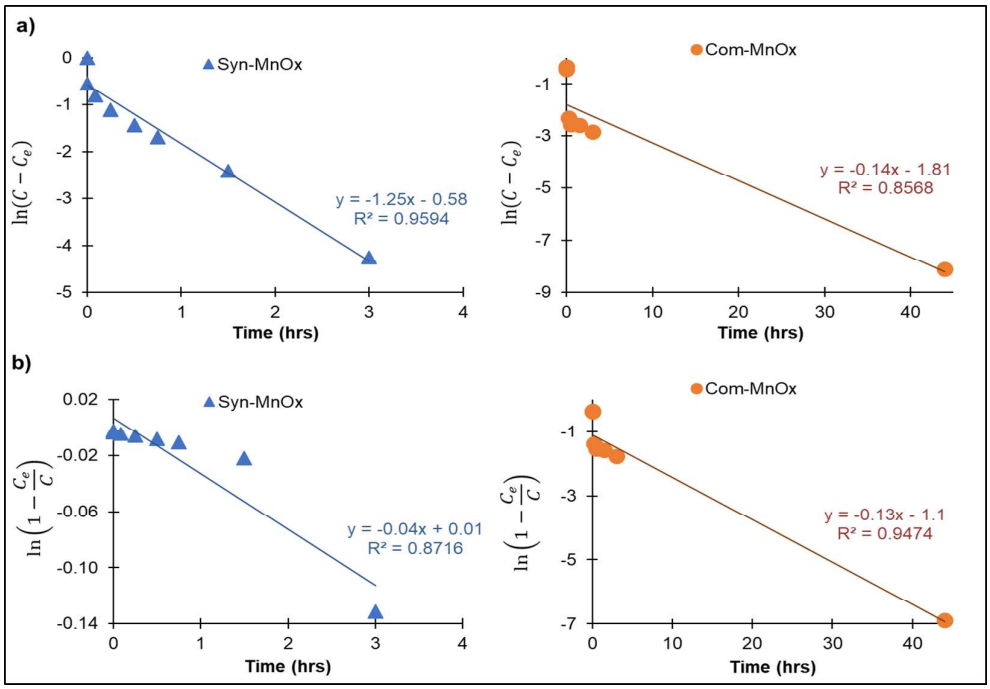

Fig. 6. Results from kinetic modelling for (a) the electron transfer limited model and (b) the surface complex formation limited model. The data points for Syn-MnO_x (triangle) and Com-MnO_x (circle) are calaculated based on the experimental data; the model fits equation and corresponding R^2 values are shown with each fit.

inhibitory effect on $MnO_{x(s)}$ reactivity due to higher points of zero charge (pH_{pzc} 6 to 9 compared to 2.4 for MnO_x) and hetero-aggregation on $MnO_{x(s)}$ surface.[11,17] Thus, the presence of these impurities in the commercial media could occupy sites in the Com-MnO_x, inhibiting the precursor complex formation. Further investigations are necessary to elucidate the influence of the Al, Fe and Si impurities and co-occurring oxides in commercial MnO_x.

The kinetic results from this study report similar trends of decreased oxidation of BPA by $MnO_{x(s)}$ over time, as seen in previous studies.[23,29,32] The increase in reduced Mn on the surface of $MnO_{x(s)}$, observed from XPS analyses and soluble Mn in solution, contributed largely to the decreasing BPA removal rate by $MnO_{x(s)}$ due to lower Mn oxidation states and competition for reactive sites.[11,23,33] Additionally, the accumulation of oxidation by-products bound on the surface as seen from the C1s, O1s and adsorption/oxidation experiment affected the surface binding which could influence the long-term reactivity of $MnO_{x(s)}$.[6,34,35]

Conclusions

The removal of BPA occurred using both synthesized (Syn-MnO_x) and commercial (Com-MnO_x) $MnO_{x(s)}$ media, but a higher BPA removal and higher Mn release to solution was observed for Syn-MnO_x. The lower surface area and impurities (Al, Fe, and Si) in Com-MnO_x possibly caused a lower effective removal of BPA compared to Syn-MnO_x. The results of surface analysis and kinetic modelling indicate that the surface chemistry strongly influences the results of the reaction. Findings from our kinetic modeling suggest that the rate limiting step for BPA removal for Syn-MnO_x is most likely electron transfer while BPA reaction with Com-MnO_x fit the surface complex formation limited model. Integration of solution chemistry and solid chemistry data suggested that the presence of Mn(III), Mn(II), and adsorbed organic compounds (e.g., BPA parent and product compounds) on the $MnO_{x(s)}$ surface contributed to the decrease in long term BPA removal rates when compared to rapid initial oxidation rates. As most studies utilize pure lab synthesized $MnO_{x(s)}$ for removal of emerging organic micropollutants such as BPA, the results of this research suggest that differences exist in the reaction mechanism between synthesized and commercial $MnO_{x(s)}$ media. Further investigations are necessary to elucidate the influence of mineral impurities and long-term reactivity of $MnO_{x(s)}$ media with environmental relevant organic concentrations to understand the fate and transport of these micropollutants and develop effective water treatment processes.

Conflicts of interest

There are no conflicts to declare.

Acknowledgements

The authors would like to thank Diana Perales and Enrique Argeñal for their help with experiments performed for this study. Funding for this research was provided by the University of New Mexico School of Engineering Startup Fund, the National Science Foundation under New Mexico EPSCoR (Grant Number #IIA-1301346) and CREST (Grant Number #HRD-1345169). Huichun Zhang acknowledges financial support from the National Science Foundation through grant number #CBET 1236517. Any opinions, findings, and conclusions or recommendations expressed in this publication are those of the author(s) and do not necessarily reflect the views of the National Science Foundation.

References

1 A. Bielen, A. Šimatović, J. Kosić-Vukšić, I. Senta, M. Ahel, S. Babić, T. Jurina, J. J. González Plaza, M. Milaković and N. Udiković-Kolić, Negative environmental impacts of antibiotic-contaminated effluents from pharmaceutical industries, *Water Res.*, 2017, **126**, 79–87.

2 B. Petrie, R. Barden and B. Kasprzyk-Hordern, A review on emerging contaminants in wastewaters and the environment: Current knowledge, understudied areas and recommendations for future monitoring, *Water Res.*, 2015, **72**, 3–27.

3 S. Kitamura, T. Suzuki, S. Sanoh, R. Kohta, N. Jinno, K. Sugihara, S. Yoshihara, N. Fujimoto, H. Watanabe and S. Ohta, Comparative study of the endocrine-disrupting activity of bisphenol A and 19 related compounds, *Toxicol. Sci.*, 2005, **84**, 249–259.

4 M. J. Arlos, L. M. Bragg, W. J. Parker and M. R. Servos, Distribution of selected antiandrogens and pharmaceuticals in a highly impacted watershed, *Water Res.*, 2015, **72**, 40–50.

5 V. de J. Gaffney, C. M. M. Almeida, A. Rodrigues, E. Ferreira, M. J. Benoliel and V. V. Cardoso, Occurrence of pharmaceuticals in a water supply system and related human health risk assessment, *Water Res.*, 2015, **72**, 199–208.

6 D. Banerjee and H. W. Nesbitt, XPS study of reductive dissolution of birnessite by oxalate: rates and mechanistic aspects of dissolution and redox processes, *Geochim. Cosmochim. Acta*, 1999, **63**, 3025–3038.

7 A. T. Stone, Reductive dissolution of manganese(III/IV) oxides by substituted phenols, *Environ. Sci. Technol.*, 1987, **21**, 979–988.

8 H. J. Ulrich and A. T. Stone, The oxidation of chlorophenols adsorbed to manganese oxide surfaces, *Environ. Sci. Technol.*, 1989, **23**, 421–428.

9 I. Forrez, M. Carballa, H. Noppe, H. De Brabander, N. Boon and W. Verstraete, Influence of manganese and ammonium oxidation on the removal of 17α-ethinylestradiol (EE2), *Water Res.*, 2009, **43**, 77–86.

10 K. Lin, W. Liu and J. Gan, Oxidative removal of bisphenol A by manganese dioxide: efficacy, products, and pathways, *Environ. Sci. Technol.*, 2009, **43**, 3860–3864.

11 S. Taujale and H. Zhang, Impact of interactions between metal oxides to oxidative reactivity of manganese dioxide, *Environ. Sci. Technol.*, 2012, **46**, 2764–2771.

12 H. Zhang, S. Taujale, J. Huang and G.-J. Lee, Effects of NOM on oxidative reactivity of manganese dioxide in binary oxide mixtures with goethite or hematite, *Langmuir*, 2015, **31**, 2790–2799.

13 K. A. Bierlein, W. R. Knocke, J. E. Tobiason, A. Subramaniam, M. Pham and J. C. Little, Modeling manganese removal in a pilot-scale postfiltration contactor, *J. Am. Water Works Assoc.*, 2015, **107**, E109–E119.

14 J. C. J. Gude, L. C. Rietveld and D. van Halem, As(III) oxidation by MnO_2 during groundwater treatment, *Water Res.*, 2017, **111**, 41–51.

15 A. Jones and W. R. Knocke, Evaluating the role of soluble aluminum in manganese removal via MnO_x(s)-coated filtration media in drinking water treatment, *Water Res.*, 2017, **111**, 59–65.

16 B. J. Lafferty, M. Ginder-Vogel and D. L. Sparks, Arsenite oxidation by a poorly crystalline manganese-oxide 1. Stirred-flow experiments, *Environ. Sci. Technol.*, 2010, **44**, 8460–8466.

17 J. E. Grebel, J. A. Charbonnet and D. L. Sedlak, Oxidation of organic contaminants by manganese oxide geomedia for passive urban stormwater treatment systems, *Water Res.*, 2016, **88**, 481–491.

18 J. de Rudder, T. V. de Wiele, W. Dhooge, F. Comhaire and Willy Verstraete, Advanced water treatment with manganese oxide for the removal of 17α-ethynylestradiol (EE2), *Water Res.*, 2004, **38**, 184–192.

19 B. Han, M. Zhang and D. Zhao, In-situ degradation of soil-sorbed 17β-estradiol using carboxymethyl cellulose stabilized manganese oxide nanoparticles: Column studies, *Environ. Pollut.*, 2017, **223**, 238–246.

20 B. Han, M. Zhang, D. Zhao and Y. Feng, Degradation of aqueous and soil-sorbed estradiol using a new class of stabilized manganese oxide nanoparticles, *Water Res.*, 2015, **70**, 288–299.

21 M. Huguet, M. Deborde, S. Papot and H. Gallard, Oxidative decarboxylation of diclofenac by manganese oxide bed filter, *Water Res.*, 2013, **47**, 5400–5408.

22 Y. Zhang, H. Zhu, U. Szewzyk and S. U. Geissen, Removal of pharmaceuticals in aerated biofilters with manganese feeding, *Water Res.*, 2015, **72**, 218–226.

23 S. Balgooyen, P. J. Alaimo, C. K. Remucal and M. Ginder-Vogel, Structural Transformation of MnO_2 during the Oxidation of Bisphenol A, *Environ. Sci. Technol.*, 2017, **51**, 6053–6062.

24 N. Shaikh, S. Taujale, H. Zhang, K. Artyushkova, A.-M. S. Ali and J. M. Cerrato, Spectroscopic investigation of interfacial interaction of manganese oxide with triclosan, aniline, and phenol, *Environ. Sci. Technol.*, 2016, **50**, 10978–10987.

25 J. M. Cerrato, M. F. Hochella, W. R. Knocke, A. M. Dietrich and T. F. Cromer, Use of XPS to identify the oxidation state of Mn in solid surfaces of filtration media oxide samples from drinking water treatment plants, *Environ. Sci. Technol.*, 2010, **44**, 5881–5886.

26 W. R. Knocke, L. Zuravnsky and J. C. Little, Adsorptive contactors for removal of soluble manganese during drinking water treatment, *J. Am. Water Works Assoc.*, 2010, **102**, 64–75.

27 H. Zhang and C.-H. Huang, Oxidative Transformation of Triclosan and Chlorophene by Manganese Oxides, *Environ. Sci. Technol.*, 2003, **37**, 2421–2430.

28 J. M. Cerrato, W. R. Knocke, M. F. Hochella, A. M. Dietrich, A. Jones and T. F. Cromer, Application of XPS and solution chemistry analyses to investigate soluble manganese removal by MnO_x(s)-coated media, *Environ. Sci. Technol.*, 2011, **45**, 10068–10074.

29 H. Zhang, W.-R. Chen and C.-H. Huang, Kinetic modeling of oxidation of antibacterial agents by manganese oxide, *Environ. Sci. Technol.*, 2008, **42**, 5548–5554.

30 P. S. Nico and R. J. Zasoski, Mn(III) center availability as a rate controlling factor in the oxidation of phenol and sulfide on δ-MnO_2, *Environ. Sci. Technol.*, 2001, **35**, 3338–3343.

31 M. B. McBride, Adsorption and oxidation of phenolic compounds by iron and manganese oxides, *Soil Sci. Soc. Am. J.*, 1987, **51**, 1466–1472.

32 K. F. Rubert IV and J. A. Pedersen, Kinetics of oxytetracycline reaction with a hydrous manganese oxide, *Environ. Sci. Technol.*, 2006, **40**, 7216–7221.

33 E. Hu, Y. Zhang, S. Wu, J. Wu, L. Liang and F. He, Role of dissolved Mn(III) in transformation of organic contaminants: Non-oxidative versus oxidative mechanisms, *Water Res.*, 2017, **111**, 234–243.

34 A. T. Stone and J. J. Morgan, Reduction and dissolution of manganese(III) and manganese(IV) oxides by organics: 2. Survey of the reactivity of organics, *Environ. Sci. Technol.*, 1984, **18**, 617–624.

35 Q. Wang, P. Yang and M. Zhu, Structural Transformation of Birnessite by Fulvic Acid under Anoxic Conditions, *Environ. Sci. Technol.*, 2018, **52**, 1844–1853.